Journal of Science and Technology in Civil Engineering NUCE 2020. 14 (1): 28–41

MULTIDISCILINARY DESIGN OPTIMIZATION FOR AIRCRAFT WING USING RESPONSE SURFACE METHOD, GENETIC ALGORITHM, AND SIMULATED ANNEALING

Xuan-Binh Lam[a,*]

[a]*Department of Mechanics, Faculty Civil Engineering, Ho Chi Minh City University of Technology and Eduation, 01 Vo Van Ngan street, Thu Duc district, Ho Chi Minh city, Vietnam*

Article history:
Received 20/08/2019, Revised 23/10/2019, Accepted 24/10/2019

Abstract

Multidisciplinary Design Optimization (MDO) has received a considerable attention in aerospace industry. The article develops a novel framework for Multidisciplinary Design Optimization of aircraft wing. Practically, the study implements a high-fidelity fluid/structure analyses and accurate optimization codes to obtain the wing with best performance. The Computational Fluid Dynamics (CFD) grid is automatically generated using Gridgen (Pointwise) and Catia. The fluid flow analysis is carried out with Ansys Fluent. The Computational Structural Mechanics (CSM) mesh is automatically created by Patran Command Language. The structural analysis is done by Nastran. Aerodynamic pressure is transferred to finite element analysis model using Volume Spline Interpolation. In terms of optimization algorithms, Response Surface Method, Genetic Algorithm, and Simulated Annealing are utilized to get global optimum. The optimization objective functions are minimizing weight and maximizing lift/drag. The design variables are aspect ratio, tapper ratio, sweepback angle. The optimization results demonstrate successful and desiable construction of MDO framework.

Keywords: Multidisciplinary Design Optimization; fluid/structure analyses; global optimum; Genetic Algorithm; Response Surface Method.

https://doi.org/10.31814/stce.nuce2020-14(1)-03

1. Introduction

Multidisciplinary Design Optimization (MDO) [1–13] has received considerable attention in the aircraft industry. MDO encompasses an extensive research area that includes the implementation of high-fidelity analysis tools in both aerodynamic and structural fields, investigations of robust interfacing algorithms for coupling these tools and improvement of the optimization algorithms quickly predict the best performances . Scientists in this area have focused attention on three main categories, embracing the accuracy, robustness and expensiveness of the proposed algorithms for application to realistic design problems effectively. For instance, Sobieski and Haftka [1] found that sound coupling and optimization methods were shown to be extremely important since some techniques, such as sequential discipline optimization, were unable to converge to the true optimum of a coupled system. On the other hand, Wakayama [2] showed that in order to obtain realistic wing planform shapes

*Corresponding author. *E-mail address:* binhlx@hcmute.edu.vn (Xuan-Binh, L.)

with aircraft design optimization, it is necessary to include multiple disciplines in conjunction with a complete set of real-world constraints.

To develop the analysis tools, the aerospace researchers have incessantly enhanced the quality as well as the fidelity of the applied codes to predict the system responses. Walsh et al. [3], for example, investigated the progresses of High-Speed Civil Transport (HSCT) design in detail. Originally, the HSCT2.1 design was realized by using low-fidelity analysis tools. A panel code with a low number of grid points was combined with an equivalent laminated plate analysis code to progress with design optimization. Meanwhile, HSCT3.5 was a multidisciplinary application that integrated medium-fidelity analysis tools, including a marching Euler code and a finite element analysis code with a limited number of mesh points. In the HSCT4.0 design, high-fidelity tools, incorporating the CFL3D Navier-Stokes flow solver and the GENESIS structural analysis package, were utilized in the design process. Alternatively, Martins [4] utilized SYN107-MB Euler/Navier-Stokes Computational Fluid Dynamics (CFD) module and FESMEH Computational Structural Mechanics (CSM) module in his research of small business jet design. The high-fidelity Euler/Navier-Stokes CFD and CSM packages have correspondingly become the *state-of-the-art* analysis modules in MDO field. Besides, the flexible aerodynamic grid can be handled by using a grid generation package (Kim et al. [5]), or grid deformation algorithm WARPMB (Martins [4]).

In addition, Kamakoti [14] and Guruswamy [15] conducted a statistical analysis of Fluid/Structure Interaction algorithms. A remarkable amount of interfacing techniques was enumerated correlative to their grades in application. Those were the Infinite Plate Spline (IPS), the Thin Plate Spline (TPS), the Multi-Quadratic biharmonic (MQ), the Finite Plate Spline (FPS), the Non-Uniform Rational B-Spline (NURBS) and Bilinear Interpolation (BI). The first technique is appropriate for linear analytical fluid models and modal approach structure models, while the last technique is highly suitable for the full Navier-Stokes flow solver and the three-dimensional (3D) finite element structural solver. On the other hand, Martins [4] also suggested his extrapolative techniques to transfer the interactive data during the process of aeroelastic analysis. Particularly, Hounjet and Meijer [16] evaluated elastomechanical and aerodynamic transfer methods, comprising of Surface Spline Interpolation (SSI) and Volume Spline Interpolation (VSI), for non-planar configurations. In general, these SSI and VSI methods are relatively simple, efficient and simultaneously adaptive to the conservation of virtual work. Consequently, they are widely used and become very popular interfacing algorithms in the field of aeroelasticity.

The improvement of optimization algorithms is also an active research area in aerospace design. The researchers in this area initially considered various traditional optimization methods, such as gradient-based optimization [4, 8–10], as effective tools to enhance their designs. The efficiency of gradient-based optimizer can significantly be enhanced by using Adjoint Method [4, 8–10]. Nevertheless, gradient-based is only a local optimizer hence can not determine the global optimum. Furthermore, the application of a global optimization algorithm for MDO system is a time-consuming activity and is nearly impossible to carry out in reality. Many scientists have considered imitating the design problem as a virtual problem in order to overcome the above difficulties. Imitating the design problem as a virtual problem implies approximating the problem to be designed by a set of basic equations that can accurately simulate the system responses. Thus far, there have been several efficient approximation methods, such as the Response Surface Method (RSM) [5–7, 17], the Artificial Neural Networks (ANN) [18–20], the Multivariate Adaptive Regression Splines (MARS) [21], the Non-Uniform Rational B-Spline (NURBS) [22], the Extended Radial Basis Function (ERBF) [23, 24], the Kriging Method (KM) [25–31], the Support Vector Regression (SVR) [32], etc, that can successfully be applied for design optimization. According to our experience, KM, ERBF and

SVR are the *state-of-the-art* metamodelings due to their high efficiency and accuracy. After being approximated by metamodelings, the design system needs to be improved and optimized by using several famous global optimization algorithms, such as Genetic Algorithm (GA) [33–38], Simulated Annealing (SA) [38–42], Evolutionary Multiobjective Optimization Algorithms (EMOA) [43–45], etc.

In general, MDO has become an increasingly interesting research area in aerospace science. The development of computational design methods reduces the overall design costs and turn-around time for the development of aerospace technology. The use of high-fidelity tools also brings more confidence to the design. On the scope of this paper, high-fidelity analysis tools were employed to validate and improve the MDO system. The commercial CFD code FLUENT [46] and the 3D Finite Element Analysis (FEA) code NASTRAN were coupled to execute the fluid flow/structural analyses and optimization process. High-fidelity interfacing algorithms were also investigated. VSI [16], defined relying on the 3D biharmonic equation which adapts to the conservation of virtual work, is used as a load transfer module that maps the aerodynamic pressure onto structural mesh. The CFD grid can be generated by using Gridgen (Pointwise) and Catia. The CSM mesh can be managed by using Patran Command Language. Moreover, the research has utilized Response Surface Method as an approximation model to imitate the system responses precisely. The global optimization codes Genetic Algorithm and Simulated Annealing are employed to obtain global optimum.

2. Fluid flow analysis and structural analysis

In this article, the simple flow diagram is implemented and is shown in detail in Fig. 1.

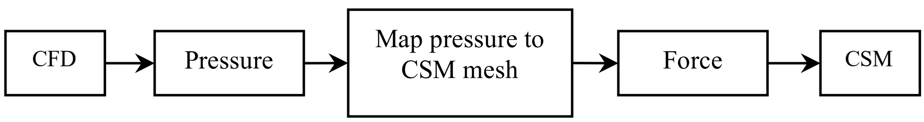

Figure 1. Fluid/Structure analyses

This is a process that connects five principal modules together, involving CFD, CSM, CFD grid generation, CSM mesh generator and data transfer (implying load transfer) modules. For each of iteration, it is necessary to map the surface loads from the CFD grid system onto the structural grid to obtain the forces on the CSM mesh system, which are then used to obtain the stresses and displacements on the CSM mesh.

2.1. Aerodynamics analysis

The aerodynamic analysis package used in this paper is the commercial CFD code FLUENT [46]. FLUENT is a high-fidelity and relatively-automatic flow solver, based on Finite Volume Method [47–51], that integrates many viscous and turbulence modelings while resolving Navier-Stokes equation. It can be completely considered as an effective fluid flow analysis module for executing coupled Aero-Structural Design Optimization. In this paper, the Spalart-Allmaras viscous modeling is integrated in the design process in order to precisely predict the aerodynamic performance. The CFD grid is generated by using Gridgen (Pointwise) [52] and Catia [53].

2.2. *Structural analysis*

The process of structural analysis can be executed by a high-fidelity, fully-automatic and robust structural analysis code NASTRAN [54]. The CSM mesh is automatically created using the Patran Command Language [55].

2.3. *Data transfer*

In coupled aero-structural analyses, the information has to be exchanged between elastomechanical and unsteady aerodynamic simulation programs. The information concerns the structural deformation connected to the elastomechanical grid and aerodynamic forces connected to the aerodynamic grid. As aerodynamic and elastomechanical models are based on grids with different structures, interpolation procedures which transfer aerodynamic and elastomechanical data between the elastomechanical and aerodynamic surface grids must be developed. It is of fundamental importance that no energy is lost in this transfer. Consequently, the forces on the structural grid and the deflections on the aerodynamic grid are restricted by [16]

$$\begin{aligned} \{f^s\} &= [G_{as}]^T \{f^a\} \\ \{u^a\} &= [G_{as}] \{u^s\} \end{aligned} \tag{1}$$

which adapts to the conservation of virtual work. $\{f^s\}$, $\{f^a\}$ and $\{u^s\}$, $\{u^a\}$ are in turn forces and deflections on structural and aerodynamic mesh, while $[G_{as}]$ is the interpolation matrix. This matrix clearly depends on the shapes of both grids and must be calculated by a reliable interpolation algorithm. In keeping with the scope of this paper, a simple, effective and robust technique, termed VSI [16], is implemented. The VSI is a very simple method which does not require any additional logic and can be applied straightforwardly to any 3D data set, without drifting so far away from the original data even the original data is non-smooth. The volume spline function can be essentially defined by relying on the 3D bi-harmonic equation [16]

$$h = d_0 + \sum_{m=1}^{N^{s+}} d_m E_m \tag{2}$$

where $E_m = \sqrt{(x^a - x^s)^2 + (y^a - y^s)^2 + (z^a - z^s)^2}$, N^{s+} is the number of structural points together with one additional constraint, (x^a, y^a, z^a) denotes the coordinates of the aerodynamic points, and (x^s, y^s, z^s) denotes the coordinates of the structural points.

The coefficients d_m can be determined from the equations of equilibrium [16]

$$\begin{aligned} &\sum_{m=1}^{N^{s+}} d_m = 0 \\ &d_0 + \sum_{m=1}^{N^{s+}} d_m E_m = h^l, \quad l = 1, ..., N^{s+} \end{aligned} \tag{3}$$

To utilize this algorithm, a prolongation matrix $[G^*]$ has to be constructed [16]

$$[G^*] = [A]\,[C]^{-1} \tag{4}$$

where

$$[C] = \begin{bmatrix} 0 & 1 & 1 & \cdots & 1 \\ 1 & E^s_{11} & E^s_{12} & \cdots & E^s_{1N^{s+}} \\ 1 & E^s_{21} & E^s_{22} & \cdots & E^s_{2N^{s+}} \\ \vdots & \vdots & \vdots & \ddots & \vdots \\ 1 & E^s_{N^{s+}1} & E^s_{N^{s+}2} & \cdots & E^s_{N^{s+}N^{s+}} \end{bmatrix} \tag{5}$$

and

$$[A] = \begin{bmatrix} 1 & E^a_{11} & E^a_{12} & \cdots & E^a_{1N^{s+}} \\ 1 & E^a_{21} & E^a_{22} & \cdots & E^a_{2N^{s+}} \\ \vdots & \vdots & \vdots & \ddots & \vdots \\ 1 & E^a_{N^a1} & E^a_{N^a2} & \cdots & E^a_{N^aN^{s+}} \end{bmatrix} \tag{6}$$

with

$$E^s_{lm} = \sqrt{(x_l - x_m)^2 + (y_l - y_m)^2 + (z_l - z_m)^2} \tag{7}$$

and

$$E^a_{lm} = \sqrt{\left(x^a_l - x_m\right)^2 + \left(y^a_l - y_m\right)^2 + \left(z^a_l - z_m\right)^2} \tag{8}$$

Finally, the interpolation matrix $[G_{as}]$ is obtained from $[G^*]$ by deleting the first column [16]

$$[G^*] = \begin{bmatrix} 0 & G_{as} \end{bmatrix} \tag{9}$$

3. Optimization algorithms

3.1. Response surface method

Many scientists have been very familiar with efficient Response Surface Method (RSM) [5–7, 17], a second-order Polynomial Regression method. The RSM is basically composed of three main elements, involving Design of Experiment (DOE), Analysis of Regression (AOR) and ANalysis of VAriance (ANOVA). RSM employs these statistical processes producing approximate functions to model the response of a numerical experiment of several independent variables. A sample quadratic response surface has the form of

$$\hat{y}(x) = c_0 + \sum_{j=1}^{p} c_j x_j + \sum_{j=1}^{p}\sum_{k=1}^{p} c_{jk} x_j x_k \tag{10}$$

where $\hat{y}$ is the response; x_j is the design variable number j, $1 \le j \le p$; c_0, c_j and c_{jk} are the unknown polynomial coefficients. It is easy to realize that there are total $m = (p+1)(p+2)/2$ coefficients in this quadratic polynomial; and at least n response values, $n \ge m$, must be available to be able to estimate these coefficients. Under such conditions, the problem may be rebuilt in the form of matrix notation as $Y \approx Xc$, where Y is a $[n \times 1]$ vector of observed responses, X is a $[n \times m]$ matrix of constants assumed to have rank r and c is a $[m \times 1]$ vector of unknown coefficients to be estimated. The least square solution of matrix problem $Y \approx Xc$ may be defined as $\widehat{c} = \left(X^T X\right)^{-1} X^T y$, this is the first step of regression. Besides retrieving the polynomial coefficients, the regression analysis also provides a method, called t-statistic, to measure the uncertainty of these coefficients. The t-statistic of a coefficient is the ratio of that coefficient value to its standard deviation. Consequently, coefficients with low values of t-statistic are not accurately estimated. Allowing poorly estimated terms to remain in the experimental model may reduce the predicted accuracy. Common measurement of the utility of removing coefficients for improving the accuracy of the response surface is called adjusted ANOVA

$$R^2_{adj} = 1 - \frac{\text{SSE}/\text{DOF}_{\text{SSE}}}{\text{SYY}/\text{DOF}_{\text{SYY}}} \tag{11}$$

where SSE is error sum of squares, SYY is total sum of squares and DOF (degree of freedom) is the number of numerical experiments. DOF_{SSE} and DOF_{SYY} are obtained from ANOVA calculations. Typical values of R^2_{adj} are from 0.9 to 1.0 when observed responses are accurately predicted.

3.2. Design of experiments

The article utilizes Central Composite Experimental Design (CCD) [56]. The central composite design sampling method is widely used in response surface applications. By selecting corner, axial, and centerpoints, it is an ideal solution for fitting a second-order response surface model. However, as it requires a relatively large number of sample points, the CCD method should only be chosen in a later stage of the RSM application when the total number of important variables is reduced to an acceptable figure. For example, a type III second-order model is proposed for a two-random-variable response surface problem and the CCD method is chosen to select the sample points. In terms of the coded variables, the design will have four runs at the corners of the square $(-1,-1), (1,-1), (-1,1), (1,1)$; one run at the center point $(0,0)$; and another four axial runs at $(-2,0), (2,0), (0,-2), (0,2)$. The total number of sample points selected for fitting such a type III model is 9 (determined by the equation $2k + 2k + 1$),10 while the minimum number of runs for fitting such model, in a saturated sampling method, is 5 (determined by the equation $2k + 1$). Thus when k is relatively large, the computational cost of running a finite element program using the CCD method is considerably higher.

3.3. Genetic algorithm

Genetic Algorithm (GA) [33–38] is a search algorithm based on the mechanics of natural selection and natural genetics, known as Darwinian's principle. A traditional GA may be essentially composed of three basic operators:

(1) Reproduction or selection: The reproduction is a process in which individual strings are copied according to their objective function values ("fitness"). Copying strings according to their fitness means that strings with higher value have a higher probability of contributing one or more offspring in the next generation. This operator is very similar to natural selection, survival of the fittest among string creatures. The reproduction may be done in a number of ways, but the easiest one is spinning a typical roulette wheel.

(2) Crossover: Members of the newly reproduced strings in the mating pool are mated at random and cross over their chromosomes together. For instance, the parents "abcde" and "ABCDE" can create an offspring with a possible chromosome "abcDE". The position between "c" and "D" is determined as crossover point where the chromosome set of the second parent overwrites the chromosome set of the first parent.

(3) Mutation: The mutation operator helps changing the state of some linking points on the parent's chromosome in order to prevent from loosing potentially useful genetic material (1's or 0's at particular locations).

Generally, a GA with an initial n-population chosen from a random selection of parameters in the parametric space. Each parameter set presents the individual's chromosome. Each individual is assigned a fitness based on how well each individual's chromosome allows it to perform in its environment. Naturally, only fit individuals are selected for mating, while weak ones die off. Mated parents create their children with chromosome sets are mix of the parent's chromosomes. The process of mating and children creation is continued so as to create a fitter generation of n children; practically, this is well presented by the increase or decrease of average fitness of the population. The process of reproduction-crossover-mutation is repeated until entire population size is replenished with children. The successive generations are created until very fit individuals are obtained.

3.4. Simulated annealing

Simulated Annealing (SA) [38–42] is a robust global optimization algorithm that has been applied widely in many engineering areas. It was originally developed for optimizing discrete global optimization problems and has been modified recently so as to analyze the continuous problems. The method is reported to perform well in the presence of a large number of design variables and local optima. Based on the idea of cooling molten metal, SA particularly has the ability to discriminate between functional "gross behavior" and "finer wrinkles" by reaching an area in the function domain where a global optimum should be present. Moreover, the inherent random fluctuations in energy allow the annealing system to escape local energy optimum to achieve the global one by moving in both uphill and downhill directions. The review of traditional SA may be described as follows:

Let $f(x)$ be the function to be minimized and x be a set of n design variables x_i $(i = 1, ..., n)$ with lower bound a_i and upper bound b_i.

- Step 1: Initializing the parameters.

The required parameters may be regarded as the starting point x^k, the initial temperature T and the original function values f^k, in which k is set as 0.

- Step 2: Generating the new candidate points.

These new coordinate values are uniformly distributed in intervals centered on the corresponding coordinate x_i using a typical neighborhood analysis. This phase will finish as soon as the points belonging to the definite domain are successfully created.

- Step 3: Accepting or rejecting the fresh candidate points relying on the Metropolis criterion.

The new state is naturally accepted if the energy of the new state is no greater than that of the current state; otherwise, it will be only accepted with probability [37–40]

$$p(\Delta f) = \exp(-\Delta f / T) \tag{12}$$

in which $\Delta f = f\left(x^{k+1}\right) - f\left(x^k\right)$, x^{k+1} is the new generated point and x^k is the original point.

In practice, a pseudo random number $p' \in [0, 1]$ is created to check the regularity of the high energy point. This point is only accepted if $p' < p$, x is updated with x' and the algorithm moves uphill. Otherwise, the point will be rejected. In case of rejection, the process returns to Step 2 to find a better candidate.

- Step 4: Reducing the temperature T.

The SA algorithm usually starts at high temperature T and maintains the tendency of slowly decreasing this parameter to reach to a low energy state. After annealing, it is necessary return Step 2 to continue reaching the optimum point.

- Step 5: Verifying the convergent condition.

The optimization process is stopped at a temperature low enough that no more useful improvements can be expected. If the convergent condition is not satisfied, it is again necessary to return to Step 2 to perform a new optimization system.

- Step 6: Exporting the optimum results.

3.5. Integrated Multiobjective Optimization algorithm

In this article, a general Multiobjective Optimization algorithm, known as weighted global criterion [37, 45], is utilized. This is a scalar method that combines all objective functions to form a single function U. The most common weighted global criterion for k objectives $f_i(x)$ may be defined as follows [37, 45]:

$$U = \left\{ \sum_{i=1}^{k} \left[w_i \left(f_i(x) - f_i^0 \right) \right]^p \right\}^{1/p} \tag{13}$$

where w_i is a vector of weights typically set by the decision maker such that $\sum_{i=1}^{k} w_i = 1$ with $w_i > 0$ and p is an adjusted coefficient which is proportional to the amount of emphasis placed on minimizing the above function with the largest difference between $f_i(x)$ and the utopia point $f_i^0 = \min\{f_i(x)\}$. Practically, the set of utopia points of multiple objectives is unique and explicit for each multiobjective optimization problem. The idea of U was developed from the concept of the *Pareto optimal*. The Pareto optimal is a compromise solution which is retrieved by minimizing the Euclidian distance $D(x) = \left\{ \sum_{i=1}^{k} \left[f_i(x) - f_i^0 \right]^2 \right\}^{1/2}$ from the utopia point in the criterion space.

In practice, the major difficulty with Multiobjective Optimization algorithm is to determine the appropriate weighting factors. The final decision for these factors is normally depends on the experience of the designer; thus, it can not yield even increases in the performance at all design points reliably. In order to overcome this difficulty, an automatic design method that determines appropriate weighting factors by relying on an integrated optimizer was developed. It is shown that the different sets of weighting factors can yield different design results of multiple objectives optimization; these factors, therefore, have to be considered as additional design variables. In the proposed method, the weighting factors are integrated in a new objective function which is defined as follows

Minimize:

$$F_n = \sum_{i=1}^{k} \sum_{j>i}^{k} \left| loss_i - loss_j \right|$$
$$loss_i = \frac{f_i^0 - f_i\left(X^{opt}\right)}{f_i^0} \tag{14}$$

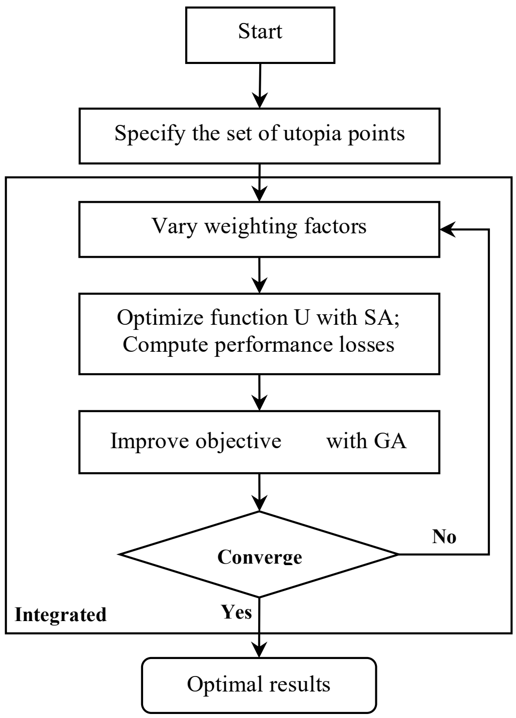

Figure 2. Design procedure of the weighting factors

The superscript opt shows the optimum point of the multiobjective function U. It is clear that X is considered as a set of design variables of multiobjective function U. w is treated as a set of design variables of the integrated objective function F_n. Practically, the $loss_i$ function indicates the performance loss of each optimized objective in comparison with its ideal point and the F_n objective function states the total mutual differences in the performance loss ratio between all optimal objectives. The set of weighting factors that minimizes the objective function F_n can improve the design evenly at all points and disciplines. The procedure for these weighting factors is summarized in the flow chart as shown in Fig. 2.

The entire process is an integration of the two optimization cycles. Firstly, the weighting factors are arbitrarily and continuously set by the integrated optimizer with the progress of the optimization process. The multiobjective function U is formed in according with each set of these factors. The optimum wing is then designed using the Simulated Annealing optimizer. After executing the wing optimization, the performance losses of all objectives, which involve the multiobjective function, are computed and used to estimate the function value of F_n to be optimized. The above process will be enhanced by the Genetic Algorithm optimizer until the convergent condition is satisfied. In general, the authors simply suggest a reasonable mode to retrieve a unique set of weighting factors relying on non-dominated solution for all objectives. No objective can dominate the others. Therefore, the design system will be improved evenly for all disciplines. However, the final decision in selection of this set of weighting factors for weighted-global-criterion objective function might depends on designer's preference in making trade-off without applying the above integrated algorithm.

4. Case study

In Vietnam, there are several optimization problems for composite cellular beam as shown in [57] and water supply system as shown in [58]. But in this article, we will do case study of design optimization problem for an aircraft wing. Wing design optimization was carried out using the proposed MDO framework. The multiobjective optimization problem was weight minimization and lift-to-drag maximization with constraint of maximum wing tip deflection. More specifically, we can see in Tables 1 and 2.

Table 1. Design variables

Design variables	Lower bound	Upper bound
Aspect ratio	3.5	4.2
Tapper ratio	0.2	0.33
Sweep angle (degrees)	31	41

Table 2. Material properties

Properties	Al 2024-T3
Elastic modulus (N/mm^2)	73100
Poisson ratio	0.33
Shear modulus (N/mm^2)	28000
Density (kg/mm^3)	2.78×10^{-6}

The airfoil of the wing is ONERA. Angle of attack is 3°. The cruising speed is 500 km/h (Mach number equals 0.4). Air density is 1.17667 kg/m^3, cruising altitude is 417 m. Fifteen experimental points were generated for 3 design variables using the CCD method. CFD and CSM analyses were performed for each of the experimental points (see Figs. 3, 4 and 5).

The response model for generating a response surface is a second-order polynomial, and 15 experimental points were generated for 3 design variables using the CCD method (see Table 3). Response surfaces were generated for the objective functions and the constraints. The generated response surfaces are optimized using the proposed integrated Multiobjective Optimization algorithm (see Table 4).

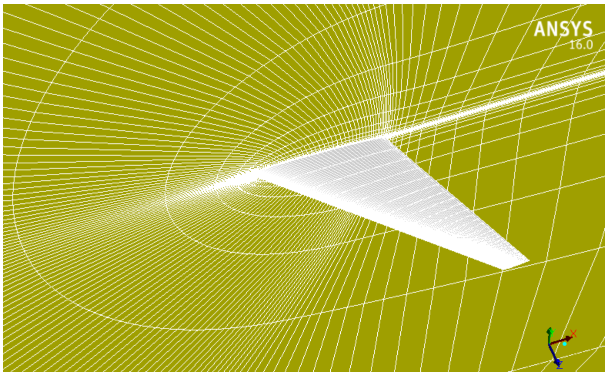

Figure 3. CFD grid generation

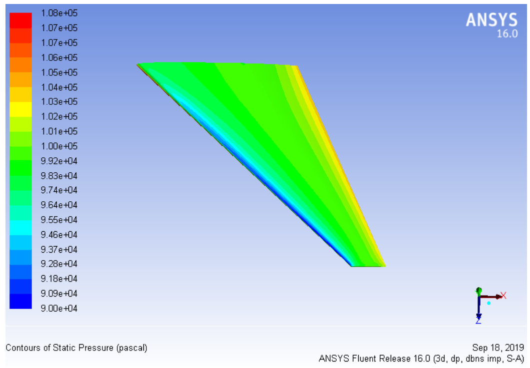

Figure 4. CFD analysis

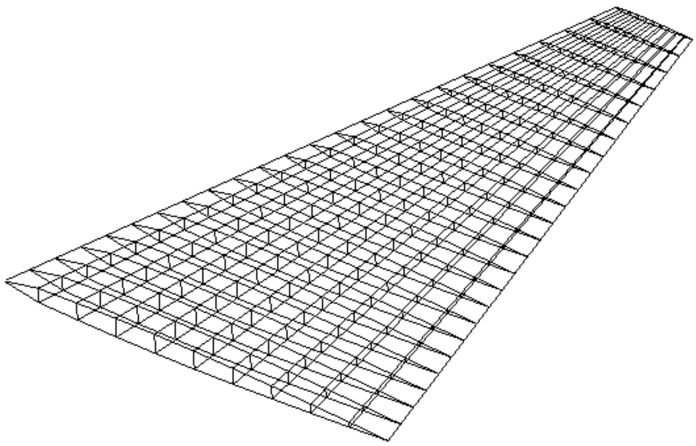

Figure 5. CSM grid generation

Table 3. Design of experiments results

Test points	Aspect ratio	Tapper ratio	Sweep angle (°C)	C_D	C_L	Mass (kg)	Deflection	Lift/Drag
1	3.85	0.265	36	0.0025008	0.14725	9.257	7.658	58.881
2	3.5	0.265	36	0.0025209	0.12947	8.530	4.638	51.359
3	3.85	0.33	36	0.0025239	0.16353	10.078	9.135	64.793
4	3.85	0.265	31	0.0025665	0.15036	9.179	5.451	58.586
5	3.85	0.265	41	0.0024960	0.14244	9.340	10.465	57.067
6	4.2	0.265	36	0.0024722	0.16506	9.986	11.904	66.766
7	3.85	0.2	36	0.0026929	0.13082	8.475	5.837	48.580
8	3.5	0.2	31	0.0027646	0.11647	7.753	2.668	42.129
9	4.2	0.2	41	0.0026939	0.14161	9.221	13.106	52.567
10	3.5	0.2	41	0.0025971	0.11218	7.877	5.269	43.194
11	4.2	0.33	31	0.0024862	0.18831	10.776	10.283	75.742
12	4.2	0.33	41	0.0025378	0.17591	10.977	19.214	69.316
13	4.2	0.2	31	0.0028076	0.14996	9.061	6.540	53.412
14	3.5	0.33	41	0.0025676	0.13949	9.364	7.653	54.327
15	3.5	0.33	31	0.0026351	0.14668	9.204	4.213	55.664

Table 4. Optimum results

Parameters	Optimized wing	Original wing
Aspect Ratio	3.78503	3.850
Tapper ratio	0.27245	0.265
Sweep angle (degrees)	34.51323	36.000
Mass (kg)	9.18909	9.257
Lift/Drag	58.51032	58.881
Lift coefficient	0.14689	0.14725

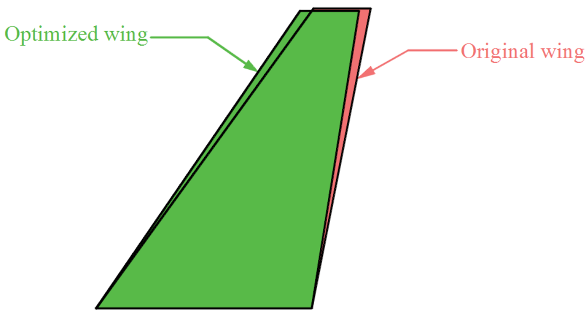

Figure 6. Optimized wing and Original wing

5. Conclusions

This research is motivated by our interest in developing and improving computational capability of MDO system. Considerable MDO work was successfully performed for a tested wing to validate several suggested algorithms that can be easily applied for more complex and practical problems. The high-fidelity structural analysis commercial code was coupled with the commercial CFD code and robust Fluid/Structure coupling algorithm to realize the analyses. The aerodynamic and structural meshes were well-managed by using Gridgen (Pointwise) and Patran Command Language. The design system was subsequently approximated by utilizing Response Surface Method. Efficient optimization algorithms (Genetic algorithm and Simulated Annealing) were used. The use of equal weighting factors does not yield even increases of performances at all design points. Thus, an automatic design method that relies on an integrated optimizer for determining appropriate weighting factors was proposed. Through the use of this method, the aerodynamic and structural performances can be improved evenly. The Multidisciplinary Aero-Structural Design is, therefore, desirable and practical.

Acknowledgement

The authors acknowledge the support of Ho Chi Minh City University of Technology and Education for major theme of the university.

References

[1] Sobieszczanski-Sobieski, J., Haftka, R. T. (1997). Multidisciplinary aerospace design optimization: survey of recent developments. *Structural Optimization*, 14(1):1–23.

[2] Wakayama, S. R. (1995). Lifting surface design using multidisciplinary optimization. PhD thesis, Stanford University.
[3] Walsh, J. L., Townsend, J. C., Salas, A. O., Samareh, J. A., Mukhopadhyay, V., Barthelemy, J.-F. (2000). Multidisciplinary high-fidelity analysis and optimization of aerospace vehicles. Part 1: Formulation. *AIAA Journal*, AIAA-2000-0418.
[4] Martins, J. R. (2002). A coupled-adjoint method for high-fidelity aero-structural optimization. PhD thesis, Stanford University.
[5] Kim, Y., Kim, J., Jeon, Y., Bang, J., Lee, D.-H., Kim, Y., Park, C. (2002). Multidisciplinary aerodynamic-structural design optimization of supersonic fighter wing using response surface methodology. In *40th AIAA Aerospace Sciences Meeting & Exhibit*, AIAA-2002-0322.
[6] Guinta, A. A. (1997). Aircraft multidisciplinary design optimization using design of experimental theory and response surface modeling methods. PhD thesis, University of Virginia.
[7] Giunta, A. A., Balabanov, V., Haim, D., Grossman, B., Mason, W. H., Watson, L. T., Haftka, R. T. (1996). Wing design for a high-speed civil transport using a design of experiments methodology. *AIAA Journal*, AIAA-96-4001.
[8] Joaquim, R. R., Alonso, J. J., Reuther, J. (2001). Aero-structural wing design optimization using high-fidelity sensitivity analysis. In *Proceeding to CEAS Conference on Multidisciplinary Aircraft Design Optimization*, Confederation of European Societies.
[9] Chittick, I. R., Martins, J. R. R. A. (2008). Aero-structural optimization using adjoint coupled post-optimality sensitivities. *Structural and Multidisciplinary Optimization*, 36(1):59–70.
[10] Gumbert, C. R., Hou, G. J.-W., Newman, P. A. (2005). High-fidelity computational optimization for 3-D flexible wings: Part I–Simultaneous aero-structural design optimization (SASDO). *Optimization and Engineering*, 6(1):117–138.
[11] Kumano, T., Jeong, S., Obayashi, S., Ito, Y., Hatanaka, K., Morino, H. (2006). Multidisciplinary design optimization of wing shape with nacelle and pylon. In *European Conference on Computational Fluid Dynamics ECCOMAS CFD*, TU Delft, The Netherlands.
[12] de Weck, O., Agte, J., Sobieszczanski-Sobieski, J., Arendsen, P., Morris, A., Spieck, M. (2007). State-of-the-art and future trends in multidisciplinary design optimization. In *48th AIAA/ASME/ASCE/AHS/ASC Structures, Structural Dynamics, and Materials Conference*, Hawaii, USA, AIAA-2007-1905.
[13] Martins, J. R. R. A., Marriage, C. (2007). An objective-oriented framework for multidisciplinary design optimization. In *48th AIAA/ASME/ASCE/AHS/ASC Structures, Structural Dynamics, and Materials Conference*, Hawaii, USA, AIAA-2007-1906.
[14] Kamakoti, R., Shyy, W. (2004). Fluid–structure interaction for aeroelastic applications. *Progress in Aerospace Sciences*, 40(8):535–558.
[15] Guruswamy, G. P. (2002). A review of numerical fluids/structures interface methods for computations using high-fidelity equations. *Computers & Structures*, 80(1):31–41.
[16] Hounjet, M. H. L., Meijer, J. J. (1995). *Evaluation of elastomechanical and aerodynamic data transfer methods for non-planar configurations in computational aeroelastic analysis*. National Aerospace Laboratory NLR.
[17] Bhadra, S., Ganguli, R. (2006). Aeroelastic optimization of a helicopter rotor using orthogonal array-based metamodels. *AIAA Journal*, 44(9):1941–1951.
[18] Bishop, C. M. (1996). *Neural networks for pattern recognition*. Oxford University Press.
[19] Haykin, S. (1999). *Neural networks: a comprehensive foundation*. Prentice-Hall International Inc, New Jersey, USA.
[20] Demuth, H. B., Beale, M. H., De Jess, O., Hagan, M. T. (1996). *Neural network design*. Massachusetts, USA.
[21] Friedman, J. H. (1991). Multivariate adaptive regression splines. *The Annals of Statistics*, 19(1):1–67.
[22] Turner, C. J., Crawford, R. H., Campbell, M. I. (2007). Multidimensional sequential sampling for NURBs-based metamodel development. *Engineering with Computers*, 23(3):155–174.
[23] Mullur, A. A., Messac, A. (2005). Extended radial basis functions: more flexible and effective metamodeling. *AIAA Journal*, 43(6):1306–1315.

[24] Mullur, A. A., Messac, A. (2006). Metamodeling using extended radial basis functions: a comparative approach. *Engineering with Computers*, 21(3):203.
[25] Koehler, J. R., Owen, A. B. (1996). *Computer experiments, Handbook of statistics 13: Design and analysis of experiments*. Elsevier Science.
[26] Giunta, A., Watson, L. (1998). A comparison of approximation modeling techniques-Polynomial versus interpolating models. *AIAA Journal*, AIAA-98-4758.
[27] Sacks, J., Welch, W. J., Mitchell, T. J., Wynn, H. P. (1989). Design and analysis of computer experiments. *Statistical Science*, 409–423.
[28] Jeong, S., Murayama, M., Yamamoto, K. (2005). Efficient optimization design method using Kriging model. *Journal of Aircraft*, 42(2):413–420.
[29] Simpson, T. W., Lin, D. K. J., Chen, W. (2001). Sampling strategies for computer experiments: design and analysis. *International Journal of Reliability and Applications*, 2(3):209–240.
[30] Simpson, T. W., Booker, A. J., Ghosh, D., Giunta, A. A., Koch, P. N., Yang, R. J. (2004). Approximation methods in multidisciplinary analysis and optimization: a panel discussion. *Structural and Multidisciplinary Optimization*, 27(5):302–313.
[31] Martin, J. D., Simpson, T. W. (2005). Use of kriging models to approximate deterministic computer models. *AIAA Journal*, 43(4):853–863.
[32] Clarke, S. M., Griebsch, J. H., Simpson, T. W. (2004). Analysis of support vector regression for approximation of complex engineering analyses. *Journal of Mechanical Design*, 127(6):1077–1087.
[33] Goldberg, D. E. (1989). *Genetic algorithms and machine learning*. Addison Wesley Longman Inc, Massachusetts, USA.
[34] Michalewicz, Z. (1996). *Genetic algorithms+ data structures = evolution programs*. Springer-Verlag Berlin Heidelberg, New York, USA.
[35] Yang, G., Reinstein, L. E., Pai, S., Xu, Z., Carroll, D. L. (1998). A new genetic algorithm technique in optimization of permanent prostate implants. *Medical Physics*, 25(12):2308–2315.
[36] Carroll, D. L. (1996). Chemical laser modeling with genetic algorithms. *AIAA Journal*, 34(2):338–346.
[37] Arora, J. S. (2004). *Introduction to optimum design*. Elsevier.
[38] Arora, J. S., Elwakeil, O. A., Chahande, A. I., Hsieh, C. C. (1995). Global optimization methods for engineering applications: A review. *Structural Optimization*, 9(3-4):137–159.
[39] Kirkpatrick, S., Gelatt, C. D., Vecchi, M. P. (1983). Optimization by simulated annealing. *Science*, 220 (4598):671–680.
[40] Goffe, W. L., Ferrier, G. D., Rogers, J. (1994). Global optimization of statistical functions with simulated annealing. *Journal of Econometrics*, 60(1-2):65–99.
[41] Corana, A., Marchesi, M., Martini, C., Ridella, S. (1987). Minimizing multimodal functions of continuous variables with the "simulated annealing" algorithm Corrigenda for this article is available here. *ACM Transactions on Mathematical Software (TOMS)*, 13(3):262–280.
[42] Yao, X. (1991). Simulated annealing with extended neighbourhood. *International Journal of Computer Mathematics*, 40(3-4):169–189.
[43] Coello, C. A. C., Lamont, G. B., Van Veldhuizen, D. A. et al. (2007). *Evolutionary algorithms for solving multi-objective problems*, volume 5. Springer.
[44] Deb, K. (2007). Current trends in evolutionary multi-objective optimization. *International Journal for Simulation and Multidisciplinary Design Optimization*, 1(1):1–8.
[45] Marler, R. T. (2005). A study of multi-objective optimization methods for engineering applications. PhD thesis, The University of Iowa.
[46] Fluent Inc (2005). *Fluent user's manual*. Fluent Inc, New Hampshire, USA.
[47] Hirsch, C. (2007). *Numerical computation of internal and external flows*. Oxford, England.
[48] Blazek, J. (2001). *Computational fluid dynamics: principles and applications*. Elsevier Science Ltd, Oxford, England.
[49] Chung, T. J. (2002). *Computational fluid dynamics*. Cambridge University Press, Cambridge, England.
[50] Ferziger, J. H., Perić, M. (2002). *Computational methods for fluid dynamics*, volume 3. Springer-Verlag Berlin Heidelberg, New York, USA.

[51] Anderson, J. D. (1995). *Computational fluid dynamics: the basics with applications*. McGraw-Hill Inc, Columbus, Ohio, USA.

[52] Pointwise Inc (2019). *Pointwise user's manual*. Pointwise Inc, USA.

[53] Dassault Systems (2019). *Catia user's manual*. Dassault Systems, France.

[54] Autodesk Inc (2019). *Autodesk inventor nastran user's manual*. Autodesk Inc, USA.

[55] MSC Software (2016). *Patran user's guide*. MSC Software, USA.

[56] Myers, R. H. (1971). *Response surface methodology*. Boston: Allyn and Bacon, Inc.

[57] Hieu, N. T., Tuan, V. A. (2018). Weight optimization of composite cellular beam based on the differential evolution algorithm. *Journal of Science and Technology in Civil Engineering (STCE)-NUCE*, 12(5): 28–38.

[58] Huong, N. L., Anh, N. V., Huyen, D. T. T., Son, T. H., Cuong, D. V. (2018). Optimization to water supply system design and operation scheme in high rise buildings. *Journal of Science and Technology in Civil Engineering (STCE)-NUCE*, 12(3):123–131.